

Superconductivity in the Bilayer Two-orbital Hubbard Model

Yao-Yuan Zheng and Wéi Wú*

School of Physics, Sun Yat-sen University, Guangzhou, Guangdong 510275, China

(Dated: December 20, 2023)

Motivated by the recently discovered high T_c nickelate superconductor $\text{La}_3\text{Ni}_2\text{O}_7$, we investigate superconductivity in a two dimensional Hubbard model on square lattice that consists of two layers of hybridizing $d_{x^2-y^2}$ and d_{z^2} orbitals. Employing cluster dynamical mean-field theory, we establish phase diagrams resolving the crucial dependence of superconducting T_c on electron hybridization V between $d_{x^2-y^2}$ and d_{z^2} orbitals at the same layer, and on hopping t_\perp between two d_{z^2} orbitals at different layers. V and t_\perp are presumably linked to the pairing phase coherence and the “pairing glue” of the system respectively. Our result in general favors a two-component theory explanation of superconductivity in a composite system. The influence of the pseudogap effect and Hund’s coupling on superconductivity are discussed, and also the implication of our result to the understanding of $\text{La}_3\text{Ni}_2\text{O}_7$ superconductivity.

Introduction - Since the discovery of heavy fermion and cuprate superconductors [1, 2], unraveling unconventional superconductivity (SC) [3–11] has been one of the thematic topics in condensed matter physics. For cuprate, despite its precise nature of d -wave pairing remains a mystery, it is widely believed that its essential physics may be captured by the single-band Hubbard model or the $t - J$ model encoding the correlation effects of the $\text{Cu-}3d_{x^2-y^2}$ electrons [6, 7]. The single-band Hubbard model also captures many other unusual phenomena of correlated electrons [5–7, 12–14], which makes it one of the most intensively studied theoretical models in condensed matter physics. It is worth noting that, many other superconductors, including the layered organic superconductor [15] and the transition metal dichalcogenides (TMDs) [16], can also be described by the single-band Hubbard model.

Very recently, novel high T_c superconductivity is reported in the pressurized nickelate $\text{La}_3\text{Ni}_2\text{O}_7$ [3, 17–23], which has a layered structure consisting of double NiO_2 planes. As revealed by the density functional theory (DFT) calculations [24–29] and experiments [30], the e_g doublet of $\text{Ni-}3d$ orbitals, *i.e.*, the $3d_{x^2-y^2}$ and $3d_{z^2}$ orbitals, are both at play in low-energy physics. The d_{z^2} orbital can be seen as more localized and near half-filled, whereas the $d_{x^2-y^2}$ orbital is near quarter-filling and in general, more itinerant [31, 32]. Electrons at two different e_g orbitals can hybridize via an intra-layer hopping V between them. The out-of-plane electron hopping t_\perp between d_{z^2} orbitals at different layers, generates an effective antiferromagnetic (AFM) coupling J_\perp deemed to be the major source of the correlation effects in the system (see Fig. 1) [32–34]. The above picture can be in general summarized as a bilayer two-orbital model [25] of $\text{La}_3\text{Ni}_2\text{O}_7$, which differs essentially from the Hubbard model of cuprates, or that of the infinite layer nickelates $R\text{NiO}_2$ ($R=\text{La,Pr,Ni}$) [35] which to be captured by the $d_{x^2-y^2}$ orbital hybridizing with less correlated $5d$ -derived bands [36–39]. It is also argued that the Hund’s coupling J_H may play an important role in

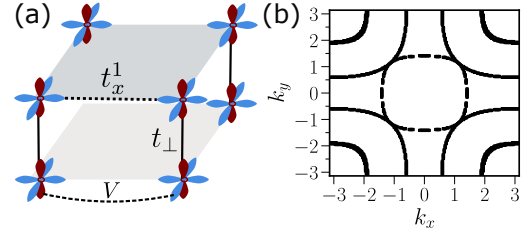


FIG. 1. Geometry and Fermi surface of the bilayer two-orbital Hubbard model on two dimensional square lattice. In subplot (a) the light symbols denote $d_{x^2-y^2}$ orbitals while dark symbols denote d_{z^2} orbitals. To plot the Fermi surface in subplot (b), $t_x^1 = -1, t_x^2 = 0.15, t_z^1 = -0.25, t_z^2 = -0.05, \mu_x = -1.6, \mu_z = -0.8, t_\perp = 1.3, V = 0.5$ are used.

$\text{La}_3\text{Ni}_2\text{O}_7$ [40–42]. All in all, the low-energy physics of $\text{La}_3\text{Ni}_2\text{O}_7$ can be sharply distinguished from previously known unconventional superconductors, which goes beyond the description of the single-band Hubbard model. A systematic study of SC in the bilayer two-orbital Hubbard (BLTO-Hubbard) model will not only shed light on comprehending $\text{La}_3\text{Ni}_2\text{O}_7$ SC, but also provide new insights into the general understanding of unconventional superconductivity.

In this work, we investigate superconductivity in BLTO-Hubbard model using cluster extensions of the dynamical mean-field theory (DMFT) [43, 44]. Performing finite temperature computations, we reveal following key aspects of SC in this system: (1) The s_\pm -wave pairing [45–55] driven by the inter-layer AFM coupling between d_{z^2} orbitals with effective $J_\perp \propto t_\perp^2/U_z$, has a non-monotonic dependence on t_\perp . In small t_\perp regime, superconducting T_c grows with t_\perp (or J_\perp), whereas at large t_\perp , T_c can be suppressed by increasing t_\perp (or J_\perp). Here U_z is the Hubbard repulsion within d_{z^2} orbital. (2) There exists a critical V_c only when the d_{z^2} - $d_{x^2-y^2}$ hybridization V greater than which the system can be superconducting. The relation between parameter V and phase coherence of pairing is discussed. (3) The calculated superconducting T_c for parameter set in relevance

to pressurized $\text{La}_3\text{Ni}_2\text{O}_7$ in general agrees with the experimental T_c [3]. Increasing V leads to higher superconducting T_c . The connection between our result and the two-component theory of superconductivity in a composite system [56–58] is discussed.

Model and method - The bilayer two-orbital Hubbard model [25] we use can be written as $H = H_0 + H_U$, which reads,

$$H_0 = -t_x^{ij} \sum_{ij\alpha\sigma} c_{i\alpha\sigma}^\dagger c_{j\alpha\sigma} - t_z^{ij} \sum_{ij\alpha\sigma} d_{i\alpha\sigma}^\dagger d_{j\alpha\sigma} - t_\perp \sum_{i\sigma\alpha} d_{i\alpha\sigma}^\dagger d_{i\bar{\alpha}\sigma} + V \sum_{\langle ij \rangle \alpha\sigma} c_{i\alpha\sigma}^\dagger d_{j\alpha\sigma} - \mu_x \sum_{i,\alpha,\sigma} n_{i\alpha\sigma}^x - \mu_z \sum_{i,\alpha,\sigma} n_{i\alpha\sigma}^z \quad (1)$$

$$H_U = U_z \sum_{i\alpha} n_{i\alpha\uparrow}^z n_{i\alpha\downarrow}^z \quad (2)$$

where t_x^{ij} , t_z^{ij} are the in-plane (or intra-layer) intra-orbital electron hoppings for $d_{x^2-y^2}$ and d_{z^2} orbitals respectively. α enumerates the two layers ($\alpha = 1, 2$) and σ indicates spin up/down. We set the in-plane hopping between the nearest neighbor (NN) sites of $d_{x^2-y^2}$ orbitals $t_x^1 \equiv t = 1$ as the energy unit throughout the paper, $t_x^1 \sim 0.48eV$ according to DFT downfolding [25]. Following which [25] the in-plane next-nearest neighbor (NNN) hopping of $d_{x^2-y^2}$ orbitals is taken as $t_x^2 = 0.15t$. The in-plane NN hopping between d_{z^2} orbitals $t_z^1 = -0.25$, and NNN hopping $t_z^2 = -0.05$. The orbital energies μ_x and μ_z can be changed to adjust the filling factors of the two e_g orbitals [32], while the total filling $n = \langle n_{i\sigma}^z + n_{i\sigma}^x \rangle = 0.75$ is fixed. The hybridization between d_{z^2} and $d_{x^2-y^2}$ orbital at the same layer V , as well as the hopping t_\perp between two d_{z^2} orbitals at the same site but different layers, will be the main controlling parameters in our study (see also Fig.1).

For the interacting part H_U , we will first consider only the Hubbard repulsion $U_z = 7$ between the d_{z^2} electrons, the more itinerant $d_{x^2-y^2}$ orbital is to be taken as non-interacting. In the end of the work, the Hubbard repulsion within $d_{x^2-y^2}$ orbital U_x , inter-orbital Hubbard U_{xz} , as well as a longitudinal Hund's coupling J_H will be considered.

The cluster DMFT methods have been extensively used in studying cuprates and related problems for they can effectively capture temporal and short-ranged spatial correlations [44, 59]. Depending on the boundary conditions of the effective cluster, there can be dynamical cluster approximation (DCA) and cellular DMFT (CDMFT) variations [44]. As we will show below, our results using different clusters converge rapidly against cluster size, demonstrating unambiguously the solidness of the cluster DMFT methods on computing T_c in this system. We will use the continuous time quantum Monte Carlo (CTQMC) [60] as impurity solver. For cases with

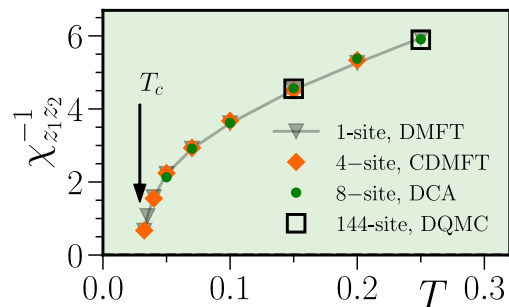


FIG. 2. Inverse of the inter-layer $d_{z^2} - d_{z^2}$ component of the s_\pm -wave pairing susceptibility, $[\chi_{z1,z2}]^{-1}$ as a function of temperature T . The temperature where $[\chi_{z1,z2}]^{-1} \rightarrow 0$ is defined as the superconducting transition T_c (black arrow). Here $U_z = 7, n_z = 0.47, n_x = 0.28, t_\perp = 0.8, V = 0.5$. HFQMC impurity solver is used here.

severe sign problem, as will be explicitly stated, Hirsch-Fye quantum Monte Carlo (HFQMC) impurity solver is also used. We have carefully verified that the two impurity solvers give the same result. Determinant quantum Monte Carlo (DQMC) is also employed to benchmark our cluster DMFT result at high temperatures.

Pairing susceptibility- For a multi-band system, different components of the pairing susceptibility simultaneously diverge as approaching superconducting T_c [61]. Without loss of generality, here we select a $d_{z^2}-d_{z^2}$ component of the pairing susceptibility, $\chi_{z1,z2}$, in which the dominant branch of the s_\pm wave pairing is found (see discussion below), to identify the pairing T_c ,

$$\chi_{z1,z2} = \frac{1}{N} \sum_{i,j} \int_0^\beta \langle \mathcal{T}_\tau p_j^\dagger(\tau) p_i(0) \rangle d\tau \quad (3)$$

where p_i is the on-site inter-layer spin-singlet pairing operator $p_i = 1/\sqrt{2}(d_{i,1,\uparrow}d_{i,2,\downarrow} - d_{i,1,\downarrow}d_{i,2,\uparrow})$ of the d_{z^2} orbital. Fig. 2 plots the inverse pairing susceptibility $\chi_{z1,z2}^{-1}$ as a function of temperature T for d_{z^2} , $d_{x^2-y^2}$ orbital being respectively close to half-, and quarter-filled ($n_z \sim 0.5, n_x \sim 0.25$). One sees that as lower temperature T , $\chi_{z1,z2}^{-1}$ decreases and eventually extrapolates to zero as approaching $T_c \sim 0.029$ (black arrow), indicating that the spontaneous SC instability can happen in this system. In Fig. 2, we find that different cluster DMFT schemes, including the single-site (1×4 orbitals) DMFT, four-site (4×4 orbitals) CDMFT, and eight-site (8×4 orbitals) DCA, all give results in excellent agreement with one another, which are agreed by the 144 site ($12 \times 12 \times 4$ orbitals) DQMC simulations at $T = 0.25, 0.15$. This result demonstrates that the non-local fluctuations are insignificant in the BLTO-Hubbard model in the given parameter regime, and also indicates the solidness of the cluster DMFT methods on computing T_c [59] here. This observation contrasts the cluster DMFT results of the single-band Hubbard model, where

finite-site effects are typically strong in small clusters [59].

Further decreasing temperature T , one obtains finite SC order parameter $\Delta_{ij}^{\alpha,\beta} = \langle \phi_{i\alpha\uparrow}^\dagger \phi_{j\beta\downarrow}^\dagger \rangle$, $\phi_{i\alpha\sigma}^\dagger \in \{c_{i\alpha\sigma}^\dagger, d_{i\alpha\sigma}^\dagger\}$ in real space when $T < T_c$. As shown in Table I, we find that the local inter-layer ($R_i = R_j, \alpha \neq \beta$) components overweight all other non-local ($R_i \neq R_j$) branches, suggesting that the SC can be best described as an s_{\pm} -wave pairing here, which agrees with previous studies [45, 46, 48–51, 62].

Phase diagram- We now study the dependence of T_c on the inter-layer d_{z_2} - d_{z_2} hopping t_{\perp} . In the localized and large U_z limit of d_{z_2} orbital, the effective AFM exchange J_{\perp} between the two d_{z_2} orbitals scales like $J_{\perp} \sim t_{\perp}^2/U_z$ to dominant order. As found in cuprates [11, 63], one may expect that the superconducting T_c grow with magnetic coupling J_{\perp} , or equivalently with t_{\perp} here. This is indeed what we observe in the small t_{\perp} regime in Fig. 3, where T_c for two different dopings, $n_z = 0.47$ (squares) and $n_z = 0.45$ (diamonds) are shown versus t_{\perp} . At large t_{\perp} , saying $t_{\perp} \gtrsim 0.8$ for $n_z = 0.47$, we however find that T_c decreases as increasing t_{\perp} . In other words, non-monotonic dependence of T_c on t_{\perp} (or J_{\perp}) is observed in Fig. 3. This behavior appears to resemble the superconducting dome in the BCS-BEC crossover phase diagram [64]. To gain insight into this observation, Inset of Fig. 3 compares the imaginary part of the local Green's function of the d_{z_2} orbital $-\text{Im}G_{z_1,z_1}(i\omega_n)$ for two different t_{\perp} at $n_z = 0.47$. As one can see that at large t_{\perp} ($t_{\perp} = 1.0$), the low-energy weight of the Green's function in the normal state ($T = 0.04 > T_c$) is greatly suppressed comparing to the smaller $t_{\perp} = 0.4$ case. Further analysis finds that the suppression of Green's function in the normal state at large t_{\perp} corresponds to the opening of a pseudogap in the low-energy density of states (not shown here). Verifying whether the BCS-BEC crossover theory applies in this model requires identifying the physical origin of the pseudogap, which can be done, for example, by using the fluctuation diagnostics method [13, 65] in future studies. It is worth noting that in cuprate, it is generally believed that the SC state is far from the BEC limit [66], despite the existence of pseudogap. Summarizing Fig. 3, we find the tendency that as n_z decreases, the suppression of the low-energy local Green's functions at large t_{\perp} becomes less severe, and the dome-like superconducting regime as

$\langle d_{i,z_1\uparrow}^\dagger d_{i,z_2\downarrow}^\dagger \rangle$	$\langle c_{i,x_1\uparrow}^\dagger c_{i,x_2\downarrow}^\dagger \rangle$	$\langle d_{i,z_1\uparrow}^\dagger d_{i+1,z_1\downarrow}^\dagger \rangle$	$\langle c_{i,x_1\uparrow}^\dagger c_{i+1,x_1\downarrow}^\dagger \rangle$
0.011	0.014	0.002	0.0004

TABLE I. Different components of the superconducting order parameter in real-space at $U_z = 7, n_z = 0.47, n_x = 0.28, t_{\perp} = 0.8, V = 0.5$ (same as in Fig. 2) from 4-site (2×2) CDMFT, $T = 0.025 < T_c \approx 0.029$. Here $\langle d_{i,z_1\uparrow}^\dagger d_{i,z_2\downarrow}^\dagger \rangle$ is the on-site, inter-layer, d_{z_2} orbital component, while $\langle c_{i,x_1\uparrow}^\dagger c_{i+1,x_1\downarrow}^\dagger \rangle$ denotes the intra-layer $d_{x^2-y^2}$ orbital component on nearest neighbor bond. HFQMC solver is used here.

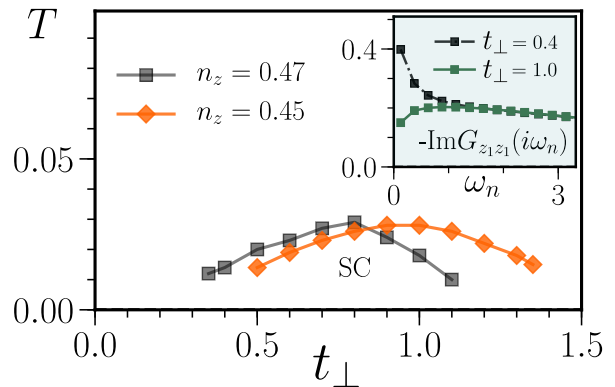


FIG. 3. Superconducting transition temperature T_c as a function of the vertical hopping amplitude t_{\perp} between two inter-layer d_{z_2} orbitals. Results for two different dopings are shown. **Inset:** Imaginary part of the local Green's function of d_{z_2} orbital $-\text{Im}G_{z_1,z_1}(i\omega_n)$ are shown as a function of Matsubara frequency ω_n for $n_z = 0.47$ at two different t_{\perp} . Here $V = 0.5, U_z = 7, n_x = 0.75 - n_z$.

a whole moves to the large t_{\perp} side.

Now we focus on how the d_{z_2} - $d_{x^2-y^2}$ hybridization V impacts on superconductivity. It is obvious that the SC instability found above cannot be attributed to the d_{z_2} orbital exclusively, though the binding of electrons does stem from the effective J_{\perp} in this orbital. Indeed, here the d_{z_2} orbital has a small intra-orbital NN hopping $t_z^{\parallel}/t = -0.25$, the Cooper pairs face difficulty in propagating coherently within the d_{z_2} plane to achieve phase ordering. The more itinerant $d_{x^2-y^2}$ orbital, on the other hand, can boost phase coherence of Cooper pairs via d_{z_2} - $d_{x^2-y^2}$ hybridization V [56, 58]. Fig. 4 displays superconducting T_c as a function of V for two different (t_{\perp}, n_z) parameter sets. It is clear in Fig. 4 that finite T_c can be obtained only when V is sufficiently large. Extrapolating T_c curve to zero T , taking the $(t_{\perp} = 0.8, n_z = 0.47)$ case for example, a critical $V_c \sim 0.4$ can be inferred for SC

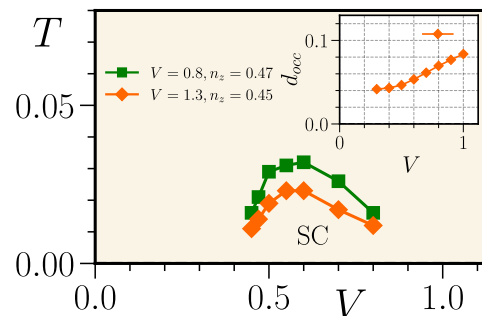


FIG. 4. Superconducting T_c as a function of V are shown for two different sets of (t_{\perp}, n_z) parameters (see also Fig. 3). **Inset:** The double occupancy $d_{occ} = \langle n_{\uparrow}^d n_{\downarrow}^d \rangle$ of d_{z_2} orbital as a function of V at $(t_{\perp} = 1.3, n_z = 0.45)$. d_{occ} increasing with V suggests the growing itinerancy of d_{z_2} orbital as V increases. Here $U_z = 7, n_x = 0.75 - n_z$.

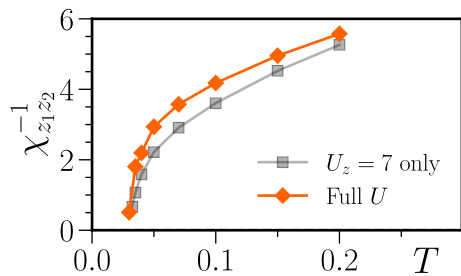


FIG. 5. Inverse pairing susceptibility, $[\chi_{z1,z2}]^{-1}$ as a function of temperature T for two different configurations of Hubbard parameters. “Full U ” denotes the case with H'_U and U_z both considered, *i.e.*, $U_x = U_z = 7$, $U_{xz} = U_z - 2J_H$, $J_H = 1.4$. Single-site DMFT and HFQMC impurity solver are used here.

instability in the zero- T limit. As for $V > V_c$, T_c grows rapidly with V , which reaches a maximum $T_c \sim 0.03$ for the $t_\perp = 0.8$ case. Further increasing V leads to, nevertheless, a suppression of T_c . This is because a large V can delocalize d_{z^2} electrons, resulting in the disruption of local d_{z^2} spin singlets and thereby being detrimental to SC. The growing itinerancy of d_{z^2} electrons with V can be manifested in the Inset of Fig.4, where double occupancy d_{occ} of d_{z^2} orbital is shown as a function of V . In Fig. 4, a different parameter set of ($t_\perp = 1.3, n_z = 0.45$) is also shown (diamonds), which exhibits similar V -dependence of T_c , suggesting the generality of our above analysis on the role of V .

It has been proposed by Yang and collaborators [50, 56] that SC in the pressurized $\text{La}_3\text{Ni}_2\text{O}_7$ fits in a two-component theory. That theory was first established by Kivelson [57, 58] to describe a “composite system” of superconductivity which can be divided into two distinct components: a “pairing” component with high pairing energy scale Δ_0 but vanishing superfluid stiffness (such as the d_{z^2} orbital here), and a “metallic” component with no pairing but high superfluid stiffness (like the $d_{x^2-y^2}$ orbital here). Berg *et al* [58] show that a high T_c can be reached approaching its mean-field value, $T_c \sim T_{MF} \approx \Delta_0/2$ if a moderate hybridization between the two components is introduced to suppress the phase fluctuations. In Fig. 2, we indeed see that in the BLTO-Hubbard model the non-local fluctuations beyond the single-site DMFT appear to be unimportant. It is also interesting to notice that here the optimal T_c is found near hybridization $V/t \approx (0.55 \sim 0.60)$ for the two parameter sets we study, which coincides with the value $V/t \sim 0.5$ obtained for the attractive Hubbard model with $U/t = -1$ [58]. One prominent difference is that, however, we find a finite critical $V_c \approx 0.4$ for SC, while in Ref. [58] SC vanishes continuously in the $V \rightarrow 0$ limit. This may be attributed to the temporal fluctuations which are treated exactly in CDMFT here, but absent in the work of Ref. [58].

Effect of U_x , U_{xz} and J_H - Above we have dis-

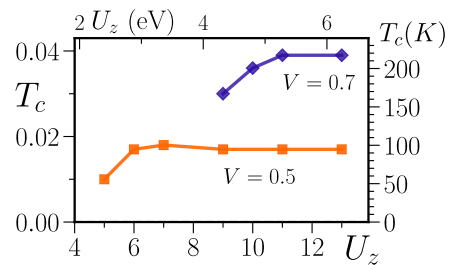


FIG. 6. Superconducting T_c as a function of U_z for two different V at fixed $t_\perp = 1.3, n_z = 0.45, n_x = 0.3$. The energy unit t_\perp^1 is set as $t_\perp^1 = 0.48\text{eV}$ as following the DFT downfolding [25].

cussed SC in the BLTO-Hubbard model considering only U_z [33]. To draw a closer connection to the realistic materials, other Hubbard parameters, including Hubbard repulsion U_x within the $d_{x^2-y^2}$ orbital, U_{xz} between the d_{z^2} and $d_{x^2-y^2}$ orbital on the same site, as well as a longitudinal Hund’s coupling J_H are considered below as, $H'_U = U_x \sum_{i\alpha} n_{i\alpha\uparrow}^x n_{i\alpha\downarrow}^x + U_{xz} \sum_{i\alpha} n_{i\alpha\uparrow}^x n_{i\alpha\downarrow}^z + (U_x - J_H) \sum_{i\alpha,\sigma} n_{i\alpha\sigma}^x n_{i\alpha\sigma}^z$. In Fig. 6, the inverse pairing susceptibility $\chi_{z1,z2}^{-1}$ as a function of T is shown to compare the results with H'_U included (diamonds), and without H'_U (only U_z , squares). As shown in which, we find that including H'_U (U_x, U_{xz} and J_H) in our study in general only modifies the T_c in a quantitative way. The superconducting state is not significantly changed. We note that a similar conclusion on the role of J_H is made by the renormalized mean-field theory study on SC in the bilayer two-orbital $t - J$ model [51]. A recent numerical study [32] on the more *ab initio* Emery-Hubbard model also finds that Hund’s coupling J_H does not affect much the magnetic correlations of the system due to the small filling factor of $d_{x^2-y^2}$ orbital.

Connection to $\text{La}_3\text{Ni}_2\text{O}_7$ and raising T_c - Finally, we discuss the connection between our result and the $\text{La}_3\text{Ni}_2\text{O}_7$ materials. For pressurized $\text{La}_3\text{Ni}_2\text{O}_7$, DFT result suggests $t_\perp \approx 1.3, V \approx 0.5$ for the BLTO-Hubbard model [25]. However, the Hubbard parameters such as U_z have not been reliably estimated. In Fig. 6 we therefore plot T_c as a function U_z while fixing $t_\perp = 1.3, V = 0.5$ (squares). One can see that as $U_z > 6$, T_c is almost independent of U_z in the U_z range we consider, suggesting a $T_c \approx 100$ Kelvin. This result in general agrees with the experimental $T_c \sim 80\text{K}$. Our study is also consistent with the absence of SC in $\text{La}_3\text{Ni}_2\text{O}_7$ under ambient pressure where d_{z^2} orbital is below the Fermi level [31]: the d_{z^2} orbital is the driving force of the composite SC. The pairing will be disabled if d_{z^2} orbital is not active at low-energies. Finally, Fig 6 shows that T_c can be considerably enhanced by increasing V if U_z is sufficiently large ($U_z \gtrsim 4\text{eV}$).

Discussion and summary - In cuprates, $d_{x^2-y^2}$ electrons act concurrently as both carrier and strongly corre-

lated medium where “pairing glue” emerges [67]. The entanglement of the two roles of electrons may be one of the reasons why cuprate SC is so difficult to understand. In pressurized $\text{La}_3\text{Ni}_2\text{O}_7$, the two active e_g orbitals may be assigned separately with those two different roles for SC. This sheds new light on comprehending unconventional superconductivity from a novel perspective. Future experiments and further theoretical studies on the BLTO-Hubbard model are warranted to confirm whether the two-component theory [56–58] provides a substantial description of the SC in $\text{La}_3\text{Ni}_2\text{O}_7$. To summarize, in this work we study superconductivity in the BLTO-Hubbard model by using cluster DMFT methods. We establish phase diagrams revealing the crucial dependence of superconducting T_c on two key physical parameters, V and t_\perp of the system. The relevance of the two-component theory of superconductivity to our results is discussed.

Acknowledgment— We thank Meng Wang, A. -M. Tremblay, Dao-Xin Yao, Changming Yue, and Xunwu Hu for useful discussions. W.W is in debt to Guang-Ming Zhang and Yi-feng Yang for discussions and suggestions. Work at Sun Yat-Sen University was supported by the National Natural Science Foundation of China (Grants No.12274472, No.11904413). To reproduce the benchmark data of this work, one can employ the open source DCA++ code (<https://github.com/CompFUSE/DCA>), with using necessary extension codes and data from (https://github.com/WUWei20/BLTO_CDMFT_benchmark)

* Corresponding author: wuwei69@mail.sysu.edu.cn

- [1] F. Steglich, J. Aarts, C. Bredl, W. Lieke, D. Meschede, W. Franz, and H. Schäfer, *Physical Review Letters* **43**, 1892 (1979).
- [2] J. G. Bednorz and K. A. Müller, *Zeitschrift für Physik B Condensed Matter* **64**, 189 (1986).
- [3] H. Sun, M. Huo, X. Hu, J. Li, Y. Han, L. Tang, Z. Mao, P. Yang, B. Wang, J. Cheng, D.-X. Yao, G.-M. Zhang, and M. Wang, *Nature* **621**, 493 (2023) (2023).
- [4] F. C. Zhang and T. M. Rice, *Phys. Rev. B* **37**, 3759 (1988).
- [5] P. A. Lee, N. Nagaosa, and X.-G. Wen, *Reviews of Modern Physics* **78**, 17 (2006).
- [6] K. Haule and G. Kotliar, *Physical Review B* **76**, 104509 (2007).
- [7] D. J. Scalapino, *Reviews of Modern Physics* **84**, 1383 (2012).
- [8] A. V. Chubukov, D. V. Efremov, and I. Eremin, *Phys. Rev. B* **78**, 134512 (2008).
- [9] B. Keimer, S. A. Kivelson, M. R. Norman, S. Uchida, and J. Zaanen, *Nature* **518**, 179 (2015).
- [10] X. Zhou, W.-S. Lee, M. Imada, N. Trivedi, P. Phillips, H.-Y. Kee, P. Törmä, and M. Erements, *Nature Reviews Physics* **3**, 462 (2021).
- [11] N. Kowalski, S. S. Dash, P. Sémon, D. Sénéchal, and A.-M. Tremblay, *Proceedings of the National Academy of Sciences* **118**, e2106476118 (2021).
- [12] B.-X. Zheng, C.-M. Chung, P. Corboz, G. Ehlers, M.-P. Qin, R. M. Noack, H. Shi, S. R. White, S. Zhang, and G. K.-L. Chan, *Science* **358**, 1155 (2017), <https://www.science.org/doi/pdf/10.1126/science.aam7127>.
- [13] W. Wú, X. Wang, and A.-M. Tremblay, *Proceedings of the National Academy of Sciences* **119**, e2115819119 (2022), <https://www.pnas.org/doi/pdf/10.1073/pnas.2115819119>.
- [14] D. P. Arovas, E. Berg, S. A. Kivelson, and S. Raghu, *Annual Review of Condensed Matter Physics* **13**, 239 (2022), <https://doi.org/10.1146/annurev-conmatphys-031620-102024>.
- [15] R. H. McKenzie, *Science* **278**, 820 (1997).
- [16] F. Wu, T. Lovorn, E. Tutuc, and A. H. MacDonald, *Phys. Rev. Lett.* **121**, 026402 (2018).
- [17] Z. Liu, H. Sun, M. Huo, X. Ma, Y. Ji, E. Yi, L. Li, H. Liu, J. Yu, Z. Zhang, *et al.*, *Science China Physics, Mechanics & Astronomy* **66**, 217411 (2023).
- [18] Y. Zhang, D. Su, Y. Huang, H. Sun, M. Huo, Z. Shan, K. Ye, Z. Yang, R. Li, M. Smidman, *et al.*, arXiv preprint arXiv:2307.14819 (2023).
- [19] J. Hou, P.-T. Yang, Z.-Y. Liu, J.-Y. Li, P.-F. Shan, L. Ma, G. Wang, N.-N. Wang, H.-Z. Guo, J.-P. Sun, *et al.*, *Chinese Physics Letters* **40**, 117302 (2023).
- [20] J. Li, C. Chen, C. Huang, Y. Han, M. Huo, X. Huang, P. Ma, Z. Qiu, J. Chen, L. Chen, T. Xie, B. Shen, H. Sun, D. Yao, and M. Wang, “Structural transition and electronic band structures in the compressed trilayer nickelate $\text{LaNi}_3\text{O}_{10}$,” (2023), arXiv:2311.16763 [cond-mat.supr-con].
- [21] Q. Li, Y.-J. Zhang, Z.-N. Xiang, Y. Zhang, X. Zhu, and H.-H. Wen, arXiv preprint arXiv:2311.05453 (2023).
- [22] T. Cui, S. Choi, T. Lin, C. Liu, G. Wang, N. Wang, S. Chen, H. Hong, D. Rong, Q. Wang, *et al.*, arXiv preprint arXiv:2311.13228 (2023).
- [23] L. Sun, Y. Zhou, J. Guo, S. Cai, P. Wang, J. Zhao, J. Han, X. Chen, Q. Wu, Y. Ding, *et al.*, arXiv preprint arXiv:2311.12361 (2023).
- [24] V. Pardo and W. E. Pickett, *Phys. Rev. B* **83**, 245128 (2011).
- [25] Z. Luo, X. Hu, M. Wang, W. Wú, and D.-X. Yao, *Phys. Rev. Lett.* **131**, 126001 (2023).
- [26] F. Lechermann, J. Gondolf, S. Bötzel, and I. M. Eremin, arXiv preprint arXiv:2306.05121 (2023).
- [27] Y. Zhang, L.-F. Lin, A. Moreo, T. A. Maier, and E. Dagotto, *Physical Review B* **108**, 165141 (2023).
- [28] B. Geisler, J. J. Hamlin, G. R. Stewart, R. G. Hennig, and P. Hirschfeld, arXiv preprint arXiv:2309.15078 (2023).
- [29] V. Christiansson, F. Petocchi, and P. Werner, *Phys. Rev. Lett.* **131**, 206501 (2023).
- [30] Z. Liu, M. Huo, J. Li, Q. Li, Y. Liu, Y. Dai, X. Zhou, J. Hao, Y. Lu, M. Wang, *et al.*, arXiv preprint arXiv:2307.02950 (2023).
- [31] J. Yang, H. Sun, X. Hu, Y. Xie, T. Miao, H. Luo, H. Chen, B. Liang, W. Zhu, G. Qu, *et al.*, arXiv preprint arXiv:2309.01148 (2023).
- [32] W. Wú, Z. Luo, D.-X. Yao, and M. Wang, arXiv preprint arXiv:2307.05662 (2023).
- [33] Y. Shen, M. Qin, and G.-M. Zhang, *Chinese Physics Letters* (2023).
- [34] S. Ryee, N. Witt, and T. O. Wehling, arXiv preprint arXiv:2310.17465 (2023).
- [35] D. Li, K. Lee, B. Y. Wang, M. Osada, S. Crossley, H. R.

- Lee, Y. Cui, Y. Hikita, and H. Y. Hwang, *Nature* **572**, 624 (2019).
- [36] Z. Wang, G.-M. Zhang, Y.-f. Yang, and F.-C. Zhang, *Phys. Rev. B* **102**, 220501 (2020).
- [37] J. Karp, A. S. Botana, M. R. Norman, H. Park, M. Zingl, and A. Millis, *Physical Review X* **10** (2020), 10.1103/physrevx.10.021061.
- [38] Y. Nomura and R. Arita, *Reports on Progress in Physics* **85**, 052501 (2022).
- [39] M. Kitatani, L. Si, P. Worm, J. M. Tomczak, R. Arita, and K. Held, *Phys. Rev. Lett.* **130**, 166002 (2023).
- [40] H. Oh and Y.-H. Zhang, arXiv preprint arXiv:2307.15706 (2023).
- [41] C. Lu, Z. Pan, F. Yang, and C. Wu, arXiv preprint arXiv:2307.14965 (2023).
- [42] Z. Liao, L. Chen, G. Duan, Y. Wang, C. Liu, R. Yu, and Q. Si, arXiv preprint arXiv:2307.16697 (2023).
- [43] A. Georges, *Reviews of Modern Physics* **68** (1996).
- [44] T. Maier, M. Jarrell, T. Pruschke, and M. H. Hettler, *Rev. Mod. Phys.* **77**, 1027 (2005).
- [45] Q.-G. Yang, D. Wang, and Q.-H. Wang, *Phys. Rev. B* **108**, L140505 (2023).
- [46] Y.-H. Tian, Y. Chen, J.-M. Wang, R.-Q. He, and Z.-Y. Lu, arXiv preprint arXiv:2308.09698 (2023).
- [47] Y. Gu, C. Le, Z. Yang, X. Wu, and J. Hu, arXiv preprint arXiv:2306.07275 (2023).
- [48] C. Lu, Z. Pan, F. Yang, and C. Wu, arXiv preprint arXiv:2310.02915 (2023).
- [49] X.-Z. Qu, D.-W. Qu, J. Chen, C. Wu, F. Yang, W. Li, and G. Su, arXiv preprint arXiv:2307.16873 (2023).
- [50] Q. Qin and Y.-f. Yang, *Phys. Rev. B* **108**, L140504 (2023).
- [51] Z. Luo, B. Lv, M. Wang, W. Wú, and D.-X. Yao, arXiv preprint arXiv:2308.16564 (2023).
- [52] H. Sakakibara, N. Kitamine, M. Ochi, and K. Kuroki, arXiv preprint arXiv:2306.06039 (2023).
- [53] Z. Pan, C. Lu, F. Yang, and C. Wu, arXiv preprint arXiv:2309.06173 (2023).
- [54] K. Jiang, Z. Wang, and F.-C. Zhang, arXiv preprint arXiv:2308.06771 (2023).
- [55] J. Chen, F. Yang, and W. Li, arXiv preprint arXiv:2311.05491 (2023).
- [56] Y.-f. Yang, G.-M. Zhang, and F.-C. Zhang, *Phys. Rev. B* **108**, L201108 (2023).
- [57] S. Kivelson, *Physica B: Condensed Matter* **318**, 61 (2002).
- [58] E. Berg, D. Orgad, and S. A. Kivelson, *Phys. Rev. B* **78**, 094509 (2008).
- [59] P. Staar, T. Maier, and T. C. Schulthess, *Phys. Rev. B* **89**, 195133 (2014).
- [60] A. N. Rubtsov, V. V. Savkin, and A. I. Lichtenstein, *Phys. Rev. B* **72**, 035122 (2005).
- [61] W. Wu and A.-M.-S. Tremblay, *Phys. Rev. X* **5**, 011019 (2015).
- [62] X.-Z. Qu, D.-W. Qu, W. Li, and G. Su, arXiv preprint arXiv:2311.12769 (2023).
- [63] W. Ruan, C. Hu, J. Zhao, P. Cai, Y. Peng, C. Ye, R. Yu, X. Li, Z. Hao, C. Jin, X. Zhang, Z.-Y. Weng, and Y. Wang, *Science bulletin* **61**, 1826 (2016).
- [64] Q. Chen, J. Stajic, S. Tan, and K. Levin, *Physics Reports* **412**, 1 (2005).
- [65] O. Gunnarsson, T. Schafer, J. P. LeBlanc, E. Gull, J. Merino, G. Sangiovanni, G. Rohringer, and A. Toschi, *Phys Rev Lett* **114**, 236402 (2015).
- [66] J. Sous, Y. He, and S. A. Kivelson, *npj Quantum Materials* **8**, 25 (2023).
- [67] T. A. Maier, D. Poilblanc, and D. J. Scalapino, *Phys. Rev. Lett.* **100**, 237001 (2008).